An Evaluation of Force-Field Treatments of Aromatic Interactions

Gianni Chessari,[a] Christopher A. Hunter,*[a] Caroline M. R. Low,[b] Martin J. Packer,[a] Jeremy G. Vinter,[b] and Cristiano Zonta[a]

Abstract: Experimental measurements of edge-to-face aromatic interactions have been used to test a series of molecular mechanics force fields. The experimental data were determined for a range of differently substituted aromatic rings using chemical double mutant cycles on hydrogen-bonded zipper complexes. These complexes were truncated for the purposes of the molecular mechanics calculations so that problems of conformational searching and the optimisation of large structures could be avoided. Double-mutant cycles were then carried out *in silico* using these truncated systems. Comparison of the experimental aromatic interaction energies and the X-ray crystal structures of these truncated complexes with the calculated data show that conventional molecular mechanics force fields (MM2, MM3, AMBER and OPLS) do not perform well. However, the XED force field which explicitly represents electron anisotropy as an expansion of point charges around each atom reproduces the trends in interaction energy and the three-dimensional structures exceedingly well. Collapsing the XED charges onto atom centres or the use of semi-empirical atom-centred charges within the XED force field gives poor results. Thus the success of XED is not related to the methods used to assign the atomic charge distribution but can be directly attributed to the use of off-atom centre charges.

Keywords: molecular modeling · pi interaction · supramolecular chemistry

Introduction

Molecular mechanics has long promised to answer major questions in molecular recognition, and recent progress in drug design, the identification of high affinity inhibitors from virtual combinatorial libraries, the characterisation of protein folding pathways and the prediction of macromolecular structure show significant headway is being made.[1–7] These developments rely on improvements in computer power, strategies for searching large structure spaces, treatment of solvent and improved force fields. The key terms in describing molecular recognition processes are clearly the non-covalent parts of the force field, but since the first molecular mechanics force fields were implemented, little has changed in the treatment of the intermolecular potential.[8, 9] A number of factors contribute to the non-covalent interaction between two molecules in solution:

1) the electrostatic interaction between the static charge distribution;
2) induction forces as a result of mutual polarisation effects;
3) van der Waals forces; and
4) desolvation.

There are several approaches to describing electrostatic interactions. The most common is based on the use of atom-centred charges (ACC). Partial charges are assigned to the nuclear centres so that the electrostatic interaction between two molecules, or between different parts of the same molecule, is then calculated as a sum of interactions using Coulomb's law. Atomic charge is not a physical observable, so it cannot be calculated in an unambiguous way using quantum mechanics. Therefore, various methods have been developed to assign ACC charges,[10–13] and there is considerable debate about the best way to define charges that reproduce experimental data best. Induction effects are difficult to take into account computationally, because they are non-additive, but their contribution in polar molecules is usually small ($<5\,\%$ of the total energy) and always favourable.[14] The van der Waals interaction results from a balance between attractive long-range forces and repulsive short-range forces. The Lennard-Jones 12-6 function describes this situation well, but others prefer to use the Morse potential.[15, 16] Solvent effects pose a particularly challenging problem, but play a major role in molecular recognition in polar solvents such as water. The

[a] Prof. C. A. Hunter, Dr. G. Chessari, Dr. M. J. Packer, C. Zonta
Centre for Chemical Biology
Krebs Institute for Biomolecular Science
Department of Chemistry, University of Sheffield
Sheffield S3 7HF (UK)
Fax: (+44) 114-273-8673
E-mail: c.hunter@sheffield.ac.uk

[b] Dr. C. M. R. Low, Dr. J. G. Vinter
James Black Foundation, 68 Half Moon Lane
Dulwich, London SE24 9JE (UK)

Supporting information for this article is available on the WWW under http://www.chemeurj.org/ or from the author.

  0947-6539/02/0813-2860 $ 17.50+.50/0

simplest approach to treating desolvation is to change the value of the dielectric constant (ε) depending on the solvent. It is also possible to use continuum solvation models (e.g. GB/SA) specific for certain solvents.[17] Calculations can also be performed inside boxes full of explicit solvent molecules.[18]

The development of good quantitative computational models for non-bonded interactions and the refinement of molecular mechanics force fields requires good quantitative experimental data against which they can be tested. There are many systematic studies based on well-designed supramolecular systems, which provide quantitative data on non-covalent interactions.[19–30] Nevertheless, the measured interactions are often strongly influenced by other factors such as neighbouring secondary interactions, cavity desolvation, or changes in geometry which are not easy to separate. In 1996, we described a new approach to measuring functional group interactions based on synthetic hydrogen-bonded complexes and the double mutant cycle concept.[31–37] The approach is illustrated in Scheme 1 for the measurement of an edge-to-face aromatic interaction. The terminal aromatic interaction of interest in complex A is fixed in an edge-to-face orientation by the rigid covalent structures of the molecules and the two hydrogen-bonding interactions. When complex A is mutated into complex B, the difference in the stability of the two complexes ($\Delta G_A - \Delta G_B$) is related not only to the aromatic interaction of interest, but also to changes in hydrogen-bond strength and other secondary interactions. All these secondary effects can be quantified by the difference $\Delta G_C - \Delta G_D$, obtained by mutation of complex C into complex D. Therefore using Equation (1), it is possible to dissect out the terminal aromatic interaction in complex A from all the other secondary effects:

$$\Delta\Delta G_{exptl} = (\Delta G_A - \Delta G_B) - (\Delta G_C - \Delta G_D) = \Delta G_A - \Delta G_B - \Delta G_C + \Delta G_D \quad (1)$$

The individual molecules are essentially rigid so that experiments are not complicated by losses of internal conformational degrees of freedom on complexation, and the free energy difference from Equation (1) reflects the enthalpy of the specific functional group interaction studied. The magnitudes of the aromatic interactions measured using this technique are remarkably sensitive to the substituents on the two aromatic rings.[38, 39] The experimental data correlate well with the Hammett substituent constants, which suggests that these differences are primarily electrostatic in origin. This data set therefore represents an ideal test bed for investigating the electrostatic term in molecular mechanics force fields. In this paper, we compare the ACC force fields available in the MacroModel package (MM2, MM3, AMBER and OPLS) with the XED force field.[40, 41] XED uses eXtended Electron Distribution points to provide a more sophisticated description of the distribution of charge around a molecule. The approach is illustrated for a carbonyl group in Figure 1: For each atom, an orbital descriptor is defined where a positive integer charge ($n+$) is allocated to the nucleus and partial negative charges are distributed on five "orbital points" or XEDs. Each XED point can be extended, retracted or eliminated according to the hybridisation type. This type of charge distribution allows us to explicitly represent the electron anisotropy associated with lone pairs and π electrons and so is expected to have a significant impact on the quality of calculations involving aromatic interactions.

Approach: Initially we focused our attention on the complete structures of the experimental complexes in Scheme 1. The three-dimensional structure of

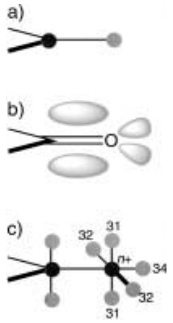

Figure 1. Representations of the charge distribution in a carbonyl group. a) The standard molecular mechanics representation uses atom-centred charges (ACCs) to reflect bond polarisation (dark grey: positive, lighter grey: negative). b) An orbital representation of the charge distribution, showing out-of-plane π-electron density and lone pairs. c) The XED representation designed to reproduce the anisotropy in electrostatic potential around each atom. A charge of $n+$ is placed at the nucleus, XED type 31 represents π-electron charges and XED types 32 and 34 represent the lone pairs. For the carbonyl carbon, the lone pair charges are zero and so are not shown. The XED charges and distances from the nucleus are listed in Table 3 according to atom type.[13]

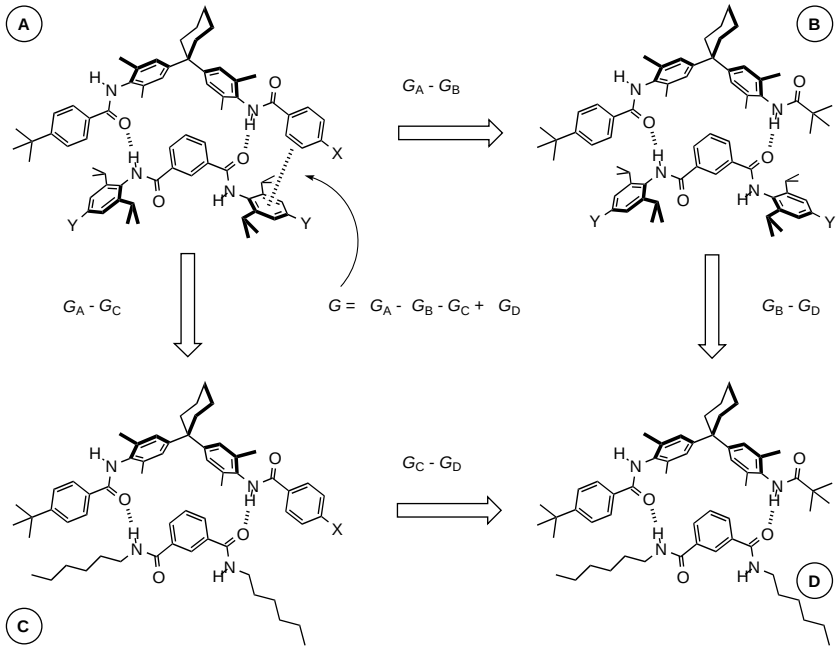

Scheme 1. The chemical double mutant cycle for experimentally determining the magnitude of the terminal aromatic interaction in complex A. Y = NO_2, H, NMe_2. X = *p*-NO_2, H, *p*-NMe_2.[31]

complex A (X = *t*Bu, Y = H) in chloroform was established using complexation-induced changes in chemical shift from ^{1}H NMR titration experiments, and a computational structure determination method developed in our laboratory.[42] However, full Monte Carlo conformational searches using four different force fields (MM2, MM3, AMBER and OPLS) failed to consistently find this structure as the global energy minimum. Only the MM3 structure matched the experimental structure. This reflects shortcomings in the force fields, which will become clear presently. Furthermore, full conformational searches would be very time consuming, if we wanted to test all nine possible X and Y substituent combinations (this operation requires the optimisation of 32 complexes for each force field as explained below).

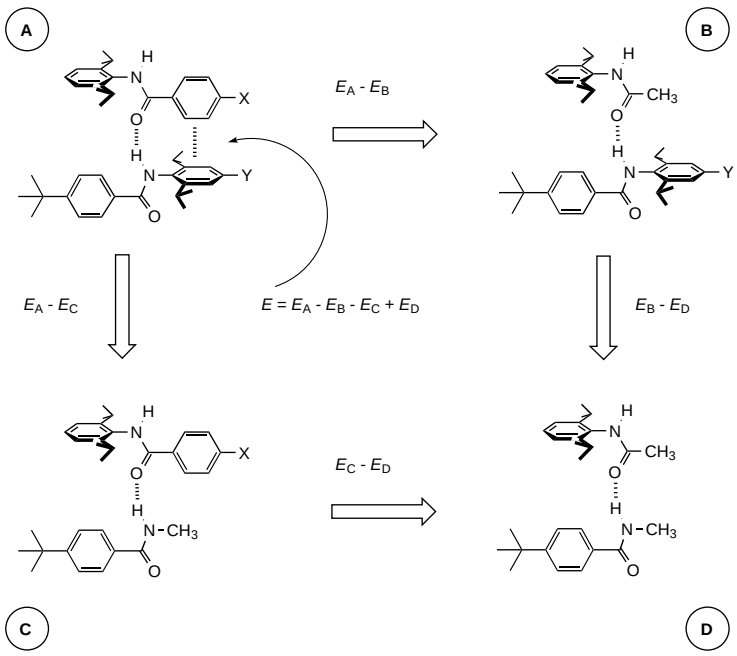

Scheme 3. The chemical double mutant cycle used to calculate the magnitude of the terminal aromatic interaction in complex A using molecular mechanics. Y = NO_2, H, NMe_2. X = *p*-NO_2, H, *p*-NMe_2.

The failure of these molecular mechanics methods to produce structures which correlate with the experimental NMR data forced us to turn to a simpler model system for which we have X-ray crystal structure data (Scheme 2a)).[43] This complex is effectively half of complex A in Scheme 1, and the hydrogen bonds and edge-to-face aromatic interactions proposed for complex A are clearly present in the dimer of **1**. The model complex **1** is characterised by two different edge-to-face interactions, and in both, the benzoyl and aniline aromatic rings are in van der Waals contact, oriented at 86° to one another. Solid state studies of a number of these dimers have shown that the geometry in the complex is unaffected by the presence of nitro and dimethylamino substituents on the aromatic rings (Scheme 2b)).[43] The approach therefore is to assume that the X-ray structure is very close to the optimum structure and simply to minimise from this starting point. This system forms the basis for the computational double mutant cycle illustrated in Scheme 3.

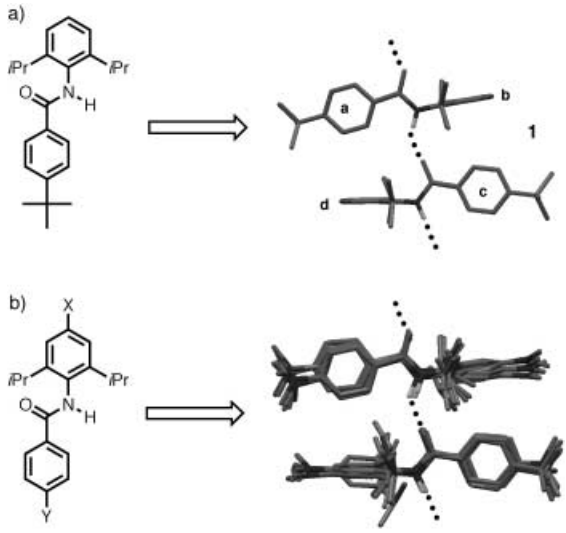

Scheme 2. The intermolecular interactions found in the X-ray crystal structures of model compound **1** (a) and an overlay of dimers from the corresponding X-ray crystal structures of a series of seven derivatives (X = H, NO_2, NMe_2 and Y = *t*Bu, NO_2, NMe_2) (b).[38] The structure of the dimer of **1** was used as a basis for constructing the complexes used in the molecular mechanics calculations by modifying aromatic rings **a**, **b**, **c** and **d** as appropriate.

A conformational analysis of the experimental system in solution has shown that each complex can adopt two conformations with different patterns of hydrogen bonds (Scheme 4a)).[33] The position of the equilibrium depends on the substituents X and Y, and the experimental ΔG values used in Equation (1) were therefore a weighted average of the ΔG values for the two conformations. We therefore considered this equilibrium in our calculations. Thus, for each complex, the α and β conformers were minimised separately, these energies were used to determine the predicted position of equilibrium, and the population-weighted average energy was used in the construction of double mutant cycles. The procedure for calculating the double mutant cycle aromatic interaction energy (ΔE) is summarised below:

1) Construct the four α conformation model complexes A–D shown in Scheme 3 by changing aromatic rings **b** and **c** in the X-ray crystal structure of the X = H, Y = *t*Bu dimer shown in Scheme 2a).
2) Construct the corresponding four β conformation complexes by changing aromatic rings **a** and **d** in the structure in Scheme 2a).
3) Find the minimum energy (E) for each of the eight complexes.

0947-6539/02/0813-2862 $ 17.50+.50/0 *Chem. Eur. J.* **2002**, *8*, No. 13

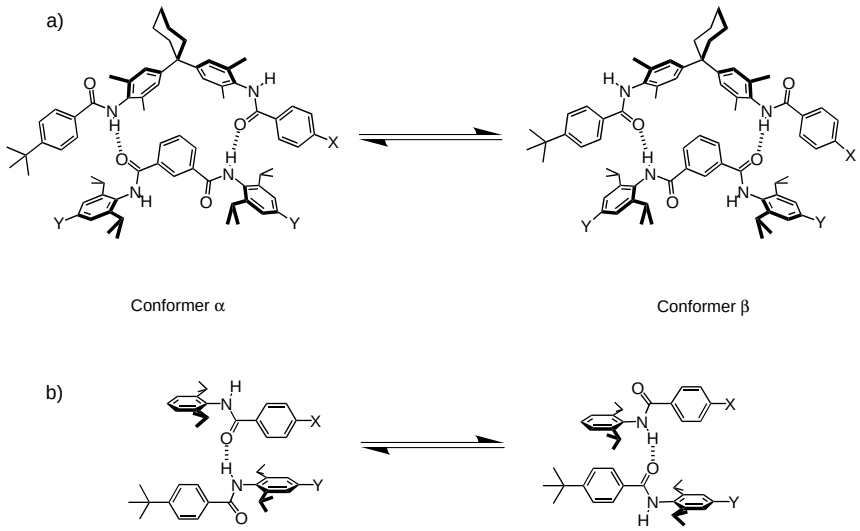

Scheme 4. Conformational equilibria in the experimentally studied complexes (a) and in the model system used in the calculations (b).

4) Calculate the populations of the α and β conformers for each complex using Equations (2) and (3).

$$\chi_\alpha = 1/\{1+\exp((E_\alpha - E_\beta)/RT)\} \quad (2)$$

$$\chi_\beta = 1-\chi_\alpha \quad (3)$$

where χ_α and χ_β are the mol fractions of conformer α and β at equilibrium.

5) Calculate the population-weighted average energy (E) for each complex using Equation (4).

$$E = \chi_\alpha E_\alpha + \chi_\beta E_\beta \quad (4)$$

6) Determine the double mutant cycle aromatic interaction energy (ΔE) using Equation (5).

$$\Delta E_{calcd} = E_A - E_B - E_C - E_D \quad (5)$$

Using this approach, all 32 complexes required to compute the nine experimental double mutant cycles were examined using the MacroModel force fields with GB/SA chloroform solvation, and the XED force field with dielectric constant two.

Computational Methods

All the calculations where run on a Silicon Graphics Indigo 2 workstation using either MacroModel 4.5 or XED.[40, 41]

Construction of complexes: Testing a force field against the experimental data from the nine double mutant cycles described in the preceding paper requires the minimisation of 32 complexes: nine pairs of complexes A (nine in the α and nine in the β conformation), three pairs of complexes B, three pairs of complexes C and one pair of complexes D. The coordinates of the dimer of **1** from the X-ray crystal structure was used with the building options in MacroModel to construct all 32 starting structures required for the minimisations. The distances and orientations of the aromatic rings and amide groups were left exactly as they were in the X-ray crystal structure of **1**, and MacroModel default bond lengths and bound angles and atom types were used to add the X and Y substituents or methyl groups. In order to avoid problems of conformational flexibility, NH_2 was used instead NMe_2 and methyl groups were used in place of *tert*-butyl and hexyl in the mutated complexes B, C and D. These simplification have no significant consequences for the double-mutant cycles. There are no direct contacts to the NMe_2 group, and its only role is polarisation of the π system. We have shown experimentally that the *tert*-butyl and methyl mutations in complexes B and D produce identical results, that is there is no *t*Bu–π interaction in this system.[31a] In all cases, NO_2 and NH_2 remained coplanar with the aromatic rings.

For the complexes A in the α conformation, the *tert*-butyl group on aromatic ring **a** and the proton *para* to the aniline nitrogen on aromatic ring **d** were replaced by the appropriate substituents X and Y (see Scheme 2a)). The same operation was performed for aromatic rings **b** and **c**, for the construction of complexes A in the β conformation. The complexes B in the α and β conformations were constructed by replacing aromatic rings **a** or **c** with methyl groups and by replacing the proton *para* to the aniline nitrogen on aromatic ring **d** or **b** with the relevant substituent Y. The complexes C in the α and β conformations were constructed by replacing aromatic rings **d** or **b** with methyl groups and by replacing the *tert*-butyl group on aromatic ring **a** or **c** with the relevant substituent X. Finally, the complexes D were obtained by substitution of aromatic rings **a** and **d** with methyl groups for the α conformer and **b** and **c** for the β conformer.

MacroModel calculations: MacroModel 4.5 versions of MM2, MM3, AMBER and OPLS force fields were tested against our experimental data.[38, 39] All the calculations were run using the following settings:

1) GB/SA continuum model was used for chloroform solvation;
2) Macromodel's BatchMin program and Polak–Ribiere conjugate gradient (*PRCG*) minimiser were used;[44]
3) 4000 iterations (It/S) were used for energy minimisation of each structure, which guaranteed complete convergence.

Equations (2)–(5) were then used to calculate the values of ΔE_{calcd} from the energies of the 32 minimised complexes.

XED calculations: XED calculations were performed using an updated version (XED98) of the original force field.[16, 41] The van der Waals parameters, XED lengths and charges are reported in Tables 1–3. The XED charge distribution is generated using a set of generic rules. The nuclear charges are determined by the number of non-bonded and π electrons associated with the atom, and the XED charges are generated using the electron distribution calculated with CHARGE3. The optimum positions of the XEDs for each atom type have been determined previously by fitting to experimental data. A new minimisation method was used. After an energy minimum was found, the program automatically removed and added all the XEDs and then the minimisation was started again. This operation was repeated until a stable minimum was found. In this way, it was possible to overcome spurious potential barriers due to the presence of complex electrostatic fields associated with XEDs and find a good reliable and reproducible minimum. The 32 complexes built with MacroModel were imported into XED, and the atom types were changed to the correct XED format: C_{ar} for aromatic carbons; C_{sp^2} for the carbonyl carbons; C_{sp^3} for aliphatic carbons; N_{tri} for amide nitrogens, for aniline nitrogens and for nitrogens in nitro groups; O_{sp^2} for carbonyl oxygens and O_{NO_2} for oxygens in nitro groups. The complexes were subjected to energy minimisation using either the XED charge distribution or the corresponding atom centred charges calculated by CHARGE3.[45] All the calculations were run using dielectric constant 2 and a maximum number of iterations of 8000, which guaranteed convergence of the minimisation.

XED was also used to perform calculations with atom centred charges derived from semi-empirical AM1 calculations.[46]

Equations (2)–(5) were then used to calculate the values of ΔE_{calcd} from the energies of the 32 minimised complexes.

Table 1. XED van der Waals parameters (E_{min} in kcal mol^{-1}).[a]

	H	C	N	O
H	0.086	0.091	0.076	0.083
C		0.129	0.121	0.134
N			0.115	0.127
O				0.140

[a] These values are appropriate for the Morse function in the XED force field. $E_{vdW} = E_{min}(z^2 - 2z)$, where $z = e^{b(1-R/Rij)}$, b = constant, R = distance between i and j, R_{ij} = sum of vdW radii.[15]

Table 2. XED van der Waals radii [Å].[a]

	H	C	N	O
H	2.760	3.030	2.750	2.970
C		3.880	3.760	3.450
N			3.330	2.700
O				2.430

Table 3. XED charge distribution lengths [Å] and charges [e].[a]

		XED type					
		Distance from nucleus [Å]			Charges [e]		
Atom type	$n+$	31	32	34	31	32	34
C sp^2	1	0.450	0.000	0.000	0.500	0.000	0.000
C ar	1	0.470	0.000	0.000	0.500	0.000	0.000
N tri	2	0.300	0.000	0.000	1.000	0.000	0.000
O sp^2	5	0.300	0.300	0.350	0.500	1.750	0.500
O NO_2	5	0.290	0.290	0.290	0.500	1.750	0.500

[a] XED type 31 represents the π-electron density and types 32 and 34 represent lone pair electron density (see Figure 1). $n+$ is the positive charge assigned to the nucleus.

Docking experiments on the dimer of **1** in Scheme 2(a) were also performed using the *XEDOCK* program to check that the X-ray structure is really the global minimum in the XED force field.

ab initio Calculations: We also attempted to investigate this sytem using ab initio methods. However using a 6-31G** basis set, the optimisation of the dimer of **1** was prohibitive in terms of computational time, and the results where not satisfactory because of the low quality of the basis set used. Generally, reliable results for non-bonded interactions can only be obtained using a basis set, which includes d orbitals.[47] Therefore, a computational study of our system can only realistically be achieved with simpler molecular mechanics models.

Structure analysis: Scheme 2b) shows that in the model compounds polarising substituents do not have a significant effect on the structures of the complexes. Consequently, the X-ray structure of **1** is a good reference structure for comparing all energy minimised complexes. Each minimised complex A was imported into XED. The two isopropyl groups, the *tert*-butyl group, the substituents X and Y and all the protons were deleted. Using the command *Fit Molecules*, the positions of the remaining cores of the complexes were compared with the structure of the corresponding core of **1**. The RMS difference between calculated and X-ray structures provides a measure of the quality of the energy minimised structure.

Results and Discussion

MM2, MM3, AMBER, OPLS, and XED were tested against the experimental edge-to-face aromatic interaction measurements using this approach. The calculated double mutant cycle energies (ΔE_{calcd}) are reported in Table 4, and the details for each complex are provided in the Supporting Information. We assume that entropy changes cancel out in the double mutant cycle, and so the experimental $\Delta\Delta G_{exptl}$ should be equivalent to the calculated functional group interaction enthalpy ΔE_{calcd}. For the XED force field, this is true (Figure 2e)). The calculated energy trend correlates well with the experimental energies ($r^2 = 0.95$), and Figure 2 shows that the force field optimised structures are very close to the X-ray structure starting point. The other force fields perform less well in terms of energy and structure (Figures 2 and 3). The MM2 and MM3 results show some correlation with the experimental energies: all the points lie in between those from the repulsive interaction due to $X = Y = NO_2$ and the

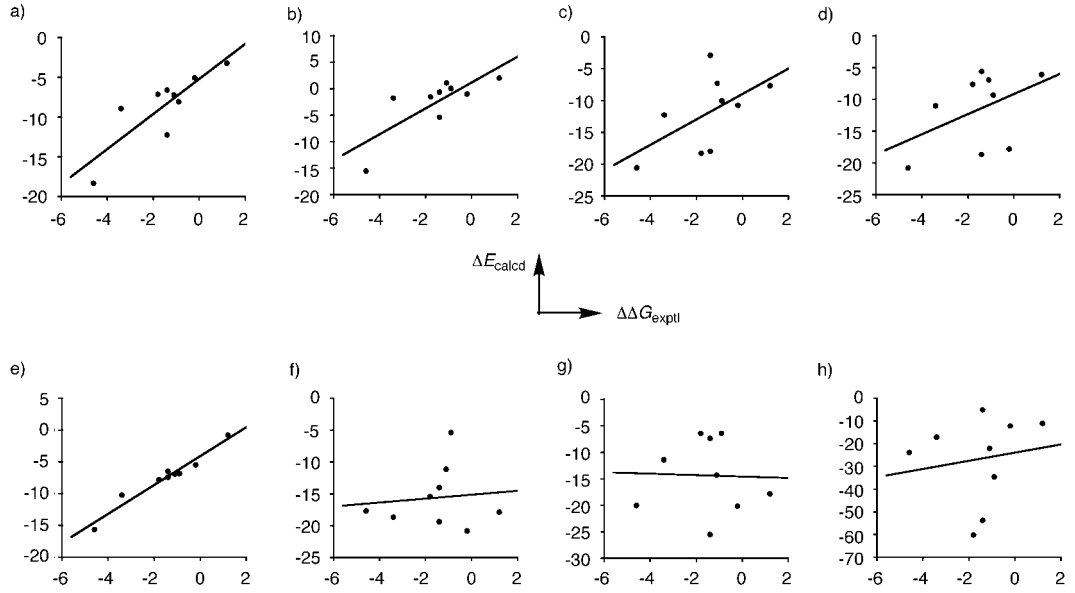

Figure 2. Comparison of the calculated molecular mechanics double mutant cycle interaction energies, ΔE_{calcd} [kJ mol^{-1}], with the experimental values, $\Delta\Delta G_{exptl}$ [kJ mol^{-1}]. The correlation coefficients (r) for the best fit straight lines shown are a) MM2 0.69, b) MM3 0.60, c) OPLS 0.33, d) AMBER 0.20, e) Standard XED 0.95, f) dielectric constant 4 in XED 0.01, g) CHARGE3 ACCs in XED 0.01, h) AM1 ACCs in XED 0.65.

0947-6539/02/0813-2864 $ 17.50+.50/0 *Chem. Eur. J.* **2002**, *8*, No. 13

Table 4. Aromatic interaction energies (ΔE_{calcd} in kJ mol^{-1}) calculated using the double mutant cycle in Scheme 3.

X	Y	MM2	MM3	AMBER	OPLS	XED	XED $\varepsilon = 4$	ACC XED CHARGE3	ACC XED AM1
NO_2	NO_2	– 3.22	2.08	– 6.08	– 7.68	– 0.82	– 17.84	– 17.83	11.09
H	NO_2	– 5.04	– 1.03	– 17.83	– 10.78	– 5.48	– 20.80	– 20.16	– 12.17
NH_2	NO_2	– 12.24	– 5.35	– 18.69	– 17.95	– 7.44	– 14.04	– 25.46	– 53.70
NO_2	H	– 8.93	– 1.78	– 11.02	– 12.27	– 10.24	– 18.64	– 11.39	– 17.04
H	H	– 6.59	– 0.66	– 5.57	– 2.90	– 6.47	– 19.38	– 7.33	– 4.99
NH_2	H	– 7.19	1.07	– 6.96	– 7.27	– 6.93	– 11.14	– 14.26	– 22.20
NO_2	NH_2	– 18.33	– 15.49	– 20.80	– 20.56	– 15.65	– 17.67	– 19.94	– 23.95
H	NH_2	– 7.12	– 1.53	– 7.63	– 18.28	– 7.77	– 15.43	– 6.35	– 60.13
NH_2	NH_2	– 8.09	0.06	– 9.33	– 10.09	– 6.88	– 5.38	– 6.38	– 34.53

strongest attraction due to X = NO_2 and Y = NH_2. The OPLS and AMBER results are far from the ideal energy trend. The poor RMS values are due to face-to-face stacking interactions in the minimised complexes rather than edge-to-face geometries.

So why does the XED force field work so well? The major difference between XED and the MacroModel force fields is the treatment of the electrostatic term in the non-covalent potential as illustrated in Figure 1. XED allows us to explicitly represent the electron anisotropy associated with lone pairs and π electrons and so might be expected to have a significant impact on the quality of calculations involving aromatic interactions. To confirm this, the sensitivity of the XED calculations to the nature of the charge distribution was investigated further. Firstly, we checked that the X-ray structure used as the starting point for the calculations really is a global minimum in the XED force field. We performed a conformational search with the XEDOCK program to dock the two monomeric units of the dimer in Scheme 2a). The lowest energy structure was very close to the X-ray structure (RMS difference in heavy atom position = 0.17 Å). Next, we investigated the use of ACCs in the XED force field. We ran one set of calculations using ACCs from CHARGE3 (this essentially collapses the XEDs onto the atomic centres) and one set of calculations with ACCs from MOPAC6 (AM1 basis set). The plots in Figure 2g) and h) show that the good correlation obtained using XED charges is lost in both cases. Also the RMS differences in structure were large, because stacking interactions were preferred to the edge-to-face orientations (Figure 3). Therefore, we conclude that the major factor that enables XED to reproduce the trend in edge-to-face aromatic interaction energies is the more sophisticated charge distribution (Figure 1).

We have so far ignored the effects of solvent on the XED calculations. The calculations were carried out using the standard dielectric constant of 2 with no explicit treatment of solvent. The effects of desolvation in chloroform are relatively small, and differences within a double-mutant cycle are probably similar across the X, Y series. However, the slope of the XED correlation plot in Figure 2 is 2.2 not 1.0, and we suspected that this reflected the influence of solvent polarity on the electrostatic interactions. That is the differences between the experimental interaction energies are damped by the dielectric of the solvent. We therefore performed the calculations again but using a dielectric constant of 4.

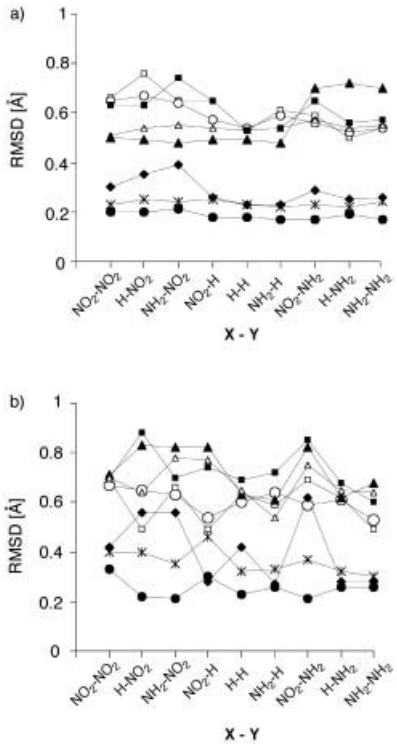

Figure 3. Comparison of the three-dimensional structures of the core of the starting point X-ray crystal structure with the cores of the complexes optimised using molecular mechanics: a) shows the data for the α conformation complexes and b) shows the data for the β conformation complexes. △ MM2, ◆ using MM3, ▲ using OPLS, □ using AMBER, ● using XED, * using XED with dielectric constant 4, □ using XED with CHARGE3 ACCs, ○ using XED with AM1 ACCs.

However, at dielectric constant 4, the XED force field did not perform well due to significant changes in the structures of the complexes (see Figures 2 and 3). This is not that surprising given that the force field was parameterised with a dielectric constant of 2, and changing this value changes the balance between the electrostatic and van der Waals contributions. We propose that the dielectric constant of 2 corresponds to the true internal dielectric for molecular surfaces which are in close contact in the complex, and the slope of the straight line in the correlation plot in Figure 2e) is related to a different effect caused by desolvating the weakly polar chloroform molecules from the interacting groups. The role of the solvent is in reducing the magnitude of the total electrostatic

interaction, but it has no effect on the relative magnitudes of the specific interactions between atoms in close contact that determine the three-dimensional structure of the interaction interface. Thus in the XED force field, a dielectric constant of 2 is appropriate for accurately predicting the three-dimensional structure of a complex and for predicting the *relative* magnitudes of the functional group interactions involved, but to quantitatively predict interaction energies, a further factor of 2 must be applied to the total electrostatic interaction to account for the effects of desolvation. It is important to note that this is not the same thing as a dielectric constant of 4 which causes a change in the structure of the complex, because it alters the balance of van der Waals and electrostatic forces in the interaction interface. This hypothesis could be experimentally tested by measuring the set of aromatic interactions in another solvent.

Conclusion

These experiments clearly demonstrate that a good electrostatic description is necessary in order to model non-covalent interactions due to electron anisotropy such as aromatic interactions. The XED force field performs much better than the ACC force fields examined, because a more sophisticated treatment of electrostatic interactions reproducing multipoles arising from π electrons and lone pairs. In the MacroModel force fields, the van der Waals contribution tends to dominate, and this disproportionately favours stacked geometries. Clearly ACC force fields have been improved by fitting the electrostatic potential calculated by quantum mechanics to charges (Kollman's ESP and RESP are good examples).[48] However, in this kind of approach each molecular fragment needs to be analysed separately which is time consuming for complex molecules and unrealisable for conformationally flexible systems where the potential surface depends on the conformation. XED overcomes these drawbacks with off-atom charges that use an empirical charge generator to take into account electronegativity and electron drift through bonds. The results described above clearly demonstrate the validity of the XED philosophy.

Acknowledgement

We thank the EPSRC (C.Z.), BBSRC (M.J.P.), the University of Sheffield (G.C.), the James Black Foundation (G.C., C.Z.) and the Lister Institute (C.A.H.) for financial support.

[1] I. D. Kuntz, *Science* **1992**, *257*, 1078 – 1082.
[2] P. Y. S. Lam, P. K. Jadhav, C. J. Eyermann, C. N. Hodge, Y. Ru, L. T. Bacheler, J. L. Meek, M. J. Otto, M. M. Rayner, Y. N. Wong, C.-H. Chang, P. C. Weber, D. A. Jackson, T. R. Sharpe, S. Erickson-Viitanen, *Science* **1994**, *263*, 380 – 384.
[3] E. M. Boczko, C. L. Brooks, *Science* **1995**, *269*, 393 – 396.
[4] P. S. Charifson, *Practical application of computer-aided drug design*, Marcel Dekker, New York, **1997**.
[5] C. L. Brooks, M. Gruebele, J. N. Onuchic, P. G. Wolynes, *Proc. Nat. Acad. Sci. USA* **1998**, *95*, 11037 – 11038.
[6] *Virtual Screening*: *An Alternative or Complement to High Throughput Screening?* (Ed.: G. Klebe), Kluwer/Escom, Dordrecht, The Netherlands, **2000**.
[7] W. F. van Gunsteren, P. Burgi, C. Peter, X. Daura, *Angew. Chem.* **2001**, *113*, 363 – 367; *Angew. Chem. Int. Ed*. **2001**, *40*, 351 – 355.
[8] N. L. Allinger, U. Burkert, *Adv. Phys. Org. Chem.* **1976**, *13*, 1 – 85.
[9] N. L. Allinger, U. Burkert, *Molecular Mechanics*, ACS Monograph No. 177, **1982**.
[10] N. L. Allinger, Y. H. Yuh, J. H. Lii, *J. Am. Chem. Soc.* **1989**, *111*, 8551 – 8566.
[11] S. R. Cox, D. E. Williams, *J. Comput. Chem.* **1981**, *2*, 304 – 323.
[12] S. J. Weiner, P. A. Kollman, D. A. Case, U. C. Singh, C. Ghio, G. Alogona, S. J. Profeta, P. Weiner, *J. Am. Chem. Soc.* **1984**, *106*, 756 – 784.
[13] W. L. Jorgensen, J. Pranata, *J. Am. Chem. Soc.* **1990**, *112*, 2008 – 2010.
[14] S. K. Burt, D. Mackay, A. T. Hangler, *Theoretical Aspects of Drug Design*: *Molecular Mechanics and Molecular Dynamics* (Eds.: T. J. Perun, C. L. Propst) Marcel Dekker, New York, pp. 55 – 89.
[15] S. D. Morley, R. J. Abraham, I. S. Haworth, D. E. Jackson, M. R. Saunders, J. G. Vinter, *J. Comput. Aided Mol. Des.* **1991**, *5*, 475 – 504.
[16] J. G. Vinter, *J. Comput. Aided Mol. Des.* **1994**, *8*, 653 – 668.
[17] W. C. Still, A. Tempczyk, R. C. Hawley, T. Hendrickson, *J. Am. Chem. Soc.* **1990**, *112*, 6127 – 6129.
[18] P. Bash, U. C. Singh, R. Langridge, P. A. Kollman, *Science* **1987**, *236*, 564.
[19] F. Cozzi, M. Cinquini, R. Annunziata, T. Dwyer, J. S. Siegel, *J. Am. Chem. Soc.* **1992**, *114*, 5729 – 5733.
[20] F. Cozzi, M. Cinquini, R. Annuziata, J. S. Siegel, *J. Am. Chem. Soc.* **1993**, *115*, 5330 – 5331.
[21] E. A. Gallo, S. H. Gellman, *J. Am. Chem. Soc.* **1993**, *115*, 9774 – 9788.
[22] L. F. Newcomb, S. H. Gellman, *J. Am. Chem. Soc.* **1994**, *116*, 4993 – 4994.
[23] R. R. Gardner, L. A. Christianson, S. H. Gellman, *J. Am. Chem. Soc.* **1997**, *119*, 5041 – 5042.
[24] S. Paliwal, S. Geib, C. S. Wilcox, *J. Am. Chem. Soc.* **1994**, *116*, 4497 – 4498.
[25] E. Kim, S. Paliwal, C. S. Wilcox, *J. Am. Chem. Soc.* **1998**, *120*, 11192 – 11193.
[26] H. J. Schneider, *Chem. Soc. Rev.* **1994**, *23*, 227 – 234.
[27] J. Sartorius, H. J. Schneider, *Chem. Eur. J.* **1996**, *2*, 1446 – 1452.
[28] J. Rebek, B. Askew, P. Ballester, C. Buhr, S. Jones, D. Nemeth, K. Williams, *J. Am. Chem. Soc.* **1987**, *109*, 5033 – 5035.
[29] K. S. Jeong, J. Rebek, *J. Am. Chem. Soc.* **1988**, *110*, 3327 – 3328.
[30] S. C. Zimmerman, C. M. Vanzyl, G. S. Hamilton, *J. Am. Chem. Soc.* **1989**, *111*, 1373 – 1381.
[31] H. Adams, F. J. Carver, C. A. Hunter, J. C. Morales, E. M. Seward, *Angew. Chem.* **1996**, *108*, 1628 – 1631; *Angew. Chem. Int. Ed. Engl.* **1996**, *35*, 1542 – 1544.
[32] H. Adams, K. D. M. Harris, G. A. Hembury, C. A. Hunter, D. Livingstone, J. F. McCabe, *J. Chem. Soc. Chem. Commun.* **1996**, 2531 – 2532.
[33] F. J. Carver, C. A. Hunter, P. S. Jones, D. J. Livingstone, J. F. McCabe, E. M. Seward, P. Tiger, S. E. Spey, *Chem. Eur. J.* **2001**, *7*, 4854 – 4862.
[34] A. P. Bisson, F. J. Carver, C. A. Hunter, J. P. Waltho, *J. Am. Chem. Soc.* **1994**, *116*, 10292 – 10293.
[35] A. P. Bisson, F. J. Carver, D. S. Eggleston, R. C. Haltiwanger, C. A. Hunter, D. L. Livingstone, J. F. McCabe, C. Rotger, A. E. Rowan, *J. Am. Chem. Soc*. **2000**, *122*, 8856 – 8868.
[36] L. Serrano, M. Bycroft, A. R. Fersht, *J. Mol. Biol.* **1991**, *218*, 465 – 475.
[37] Y. Kato, M. M. Conn, J. Rebek, *J. Am. Chem. Soc.* **1994**, *116*, 3279 – 3284.
[38] F. J. Carver, C. A. Hunter, E. M. Seward, *Chem. Commun.* **1998**, 775 – 776.
[39] F. J. Carver, C. A. Hunter, D. J. Livingstone, J. M. McCabe, E. M. Seward, *Chem. Eur. J.* **2002**, *8*, 2847 – 2859, see preceding paper.
[40] F. Mohamadi, N. G. J. Richards, W. C. Guida, R. Liskamp, M. Lipton, C. Caufield, G. Chang, T. Hendrickson, W. C. Still, *J. Comp. Chem.* **1990**, *11*, 440 – 467.
[41] J. G. Vinter, *J. Comput. Aided Mol. Des.* **1996**, *10*, 417 – 426.
[42] C. A. Hunter, M. J. Packer, *Chem. Eur. J.* **1999**, *5*, 1891 – 1897.

  0947-6539/02/0813-2866 $ 17.50+.50/0

[43] H. Adams, P. L. Bernad, D. S. Eggleston, R. C. Haltiwanger, K. D. M. Harris, G. A. Hembury, C. A. Hunter, D. J. Livingstone, B. M. Kariuki, J. F. McCabe, *Chem. Commun.* **2001**, 1500–1501.
[44] E. Polak, G. Ribiere, *Revue Francaise Informat. Recherche Operationelle* **1969**, *16*, 17–34.
[45] R. J. Abraham, P. E. Smith, *J. Comput. Aided Mol. Des.* **1989**, *3*, 175–187 and references therein.
[46] G. Rauhut, T. Clark, *J. Comput. Chem.* **1993**, *14*, 503–509.
[47] P. W. Atkins, *Molecular Quantum Mechanics*, 6th ed., OUP, Oxford, **1998**.
[48] C. I. Bayly, P. Cieplak, W. D. Cornell, P. A. Kollman, *J. Phys. Chem.* **1993**, *97*, 10269–10280.

Received: November 6, 2001 [F3665]

  0947-6539/02/0813-2867 $ 17.50+.50/0